ILC2-derived IL-9 inhibit s colorectal cancer progression by activating CD8+ T cells

Jie Wan
Jiangsu University
Lan Huang
Jiangsu University
Yinqiu Wu
Jiangsu University
Xiaoyun Ji
Jiangsu University
Shun Yao
Sun Yat-Sen University
Mohamed Hamed Abdelaziz
Jiangsu University
Wei Cai
Jiangsu University
Huixuan Wang
Jiangsu University
Jianjun Cheng
Jiangsu University
Kesavan Dinesh kumar
Jiangsu University
Vasudevan Aparna
Jiangsu University
Caixia Sun
Jiangsu University
Zhaoliang Su
Jiangsu University
Shengjun Wang
Jiangsu University
huaxi xu (xuhx@ujs.edu.cn)

Research

Keywords: ILC2s, IL-9, colorectal cancer, CD8+ T cells, tumor inhibiting

Posted Date: April 17th, 2020

DOI: https://doi.org/10.21203/rs.3.rs-22746/v1

Version of Record: A version of this preprint was published on April 1st, 2021. See the published version at https://doi.org/10.21203/rs.3.rs-22746/v1.

Abstract

Background

Type 2 innate lymphoid cells (ILC2s), characterized by secreting type 2 cytokines, regulate multiple immune responses. ILC2s are found in different tumor tissues and ILC2-derived interleukin (IL)-4, IL-5, and IL-13 act on the cells in tumor microenvironment to participate in tumor progression. ILC2s are abundant in colorectal cancer (CRC) tissue, but the role of ILC2s in CRC remains unclear.

Methods

ILC2s were sorted from the spleen using microbeads combined with flow cytometry and tumor infiltrating $CD8^+$ T cells were isolated from tumor tissue by microbeads. Flow cytometry and immunofluorescence were used to detect the percentage of ILC2s and $CD8^+$ T cells in the spleen and CRC tissue. Effects of IL-9 and IL-9-stimulated $CD8^+$ T cells on CT26 cells were measured by proliferation, apoptosis, and migration assays in vitro. GEPIA was used to detect the ILC2s chemokines in CRC tissue and adjacent normal tissue.

Results

We found that ILC2s were increased in CRC tissue compared with the adjacent normal tissue. In vitro experiments showed that IL-9 could activate $CD8^+$ T cells to promote the death of CT26 cells. ILC2s were the main IL-9-secreting cells in CRC tissue as shown by flow cytometry analysis. In vivo experiments showed that neutralizing ILC2s promoted the tumor growth, while tumor inhibition occurred by intravenous injection of IL-9.

Conclusions

Our results demonstrated that ILC2-derived IL-9 activated $CD8^+$ T cells to promote anti-tumor effects in CRC.

Background

Colorectal cancer (CRC) is a common gastrointestinal malignant tumor with no obvious symptoms in the early stage and serious systemic symptoms such as anemia and weight loss in the advanced stage[1]. Surgical resection combined with chemotherapy and radiotherapy is the standard treatment for CRC. However, CRC patients frequently show recurrence and the long-term survival rate is poor[2]. In recent years, immunotherapy has been explored as a therapeutic treatment for CRC. Studies have shown that several immune cells modulate CRC response by infiltrating the CRC microenvironment[3, 4]. Among

these immune cells, type 2 innate lymphoid cells (ILC2s) are abundant in the gut to regulate the gut homeostasis[5, 6]. However, the role and underlying mechanism by which ILC2 involves CRC development has not been elucidated.

ILC2s, a subset of ILCs, are resident primarily in the gut mucosa, lung, adipose tissue, and skin and characterized by secreting type 2 cytokines IL-4, IL-5, IL-9, and IL-13[7–9]. ILC2s were originally found to play an important role in allergic diseases and helminth diseases by promoting the type 2 immune response[10, 11]. Recently, increasing numbers of studies have demonstrated a role for ILC2s in the regulation of tumor development and progression[12, 13]. ILC2s participate in tumor development through secretion of type 2 cytokines, including IL-4, IL-5, and IL-13. ILC2-derived IL-4 promotes tumorigenesis by activating MDSCs and polarizing macrophages towards a pro-tumorigenic M2 phenotype[14]. IL-13 secreted by ILC2s exhibits a similar function[15, 16]. In addition, ILC2-derived amphiregulin can activate Tregs to promote an immunosuppressive environment[17]. ILC2s also exhibit anti-tumorigenic activity[18]. ILC2-derived IL-5 promotes the proliferation and maturation of eosinophils, which then produce a large amount of $CD4^+$ T and $CD8^+$ T cells chemokines CXCL9, CXCL10, and CCL17, leading to the recruitment of anti-tumor T cells into the tumor microenvironment and anti-tumorigenic effects[19]. However, the role of ILC2-derived IL-9, one of the main effector cytokines of ILC2s[20], in tumors remains unclear.

IL-9 was originally identified as a T-cell growth factor that is secreted by T-helper (Th) 9 cells, ILC2s, Tc9 cells, Vδ2 T cells, and mast cells[21–24]. As a pleiotropic cytokine, IL-9 acts on T cells, B cells, mast cells, and airway epithelium cells to participate in the progression of tumors, allergic diseases[25], inflammatory diseases[26], and autoimmune diseases[27] by activating the STAT1, STAT3, and STAT5 signaling pathways[28]. IL-9 regulates the development of tumors directly or indirectly by affecting the survival of tumor cells or activating immune cells in tumors[29]. Moreover, IL-9 exerts its functions in tumors in a cancer-specific manner: IL-9 commonly promotes tumor progression in hematological neoplasms while it prevents the development of solid tumors[30, 31]. Among IL-9-secreting cells, Th9 cells are the most studied in tumors. Previous studies showed that Th9 cells inhibit the development of melanoma and breast cancer by secreting IL-9[32, 33]. In addition, Th9-derived IL-9 promotes the expansion of $CD8^+$ T cells through IL-9 receptor (IL-9R) in CRC[34]. However, the main IL-9-producing cell subset in CRC remains unclear.

Here we investigated the role of ILC2s and IL-9 in the CRC progression. The IL-9-producing cell subset in CRC tissue was also detected. We hypothesized that ILC2-derived IL-9 could exert an antitumor role in CRC.

Materials And Methods

Cell line and cell culture

The murine CRC cell line CT26 was purchased from the American Type Culture Collection (Manassas, VA, USA). Cells were cultured in a humidified incubator with 5% CO2 at 37 °C.

Animals

Female BALB/c mice (6–8 weeks, 18–22 g) were purchased from the Animal Center of Yangzhou University (Yangzhou, China) and the Animal Center of Jiangsu University (Zhenjiang, China). Mice were housed in cages and bred in pathogen-free rooms with a temperature of 23 °C ± 2 °C and relative humidity of 55%±10%. All animal experiments complied with the protocol of Jiangsu University Animal Ethics and Experimentation Committee.

CRC patient tumor tissue and frozen section

The CRC patient tissue was obtained from Department of General Surgery, Affiliated Hospital of Jiangsu University (Zhenjiang, China) and the CRC tissue and adjacent normal tissue frozen sections were obtained from the Department of Pathology, Jiangsu Cancer Hospital (Nanjing, China).

Construction of the CRC model and the CT26 cell transplantation model

To construct the CRC model, mice (6-weeks-old) received a single intraperitoneal injection of AOM (Ray Biotech, Guangzhou, China) at a dose of 10 mg/kg body weight. At 7 days after the AOM injection, mice were administered drinking water with 2% DSS (Novus, Centennial, USA) for 7 days, followed by DSS-free drinking water for 14 days. After this 21-day treatment was repeated for five cycles, the CRC mice model were sacrificed and tumor tissues were harvested for subsequent analysis.

For the CT26 transplantation model, 1×10^6 CT26 cells were implanted in mice by subcutaneous injection. Five days after CT26 transplantation, anti-CD90.2 (Biolegend, CA, USA), anti-IL-9 (Biolegend), or IL-9 (Peprotech, Rocky Hill, USA) were administrated to the CT26 cell-bearing mice to intervene the tumor growth through tail vein injection. The tumor length (L), diameter and width (W) were tested with a vernier calipers, and tumor volumes were calculated using the formula $V = \pi \times L \times W2/6$.

Isolation of $CD8^+$ T cells and ILC2s

Murine $CD8^+$ T cells were isolated from tumor tissue using the tumor infiltration $CD8^+$ T-cell magnetic bead sorting kit (Miltenyi Biotec, Belgish-Gladbach, Germany). Cell purity was confirmed by flow cytometry (96%). Sorted $CD8^+$ T cells were cultured in RPMI 1640 medium supplemented with 10% FBS (Gibco, NY, USA), 2 μg/ml anti-CD3 and anti-CD28 (Biolegend), 10 U/ml penicillin and 10 U/ml streptomycin (Gibco).

ILC2s were sorted from murine spleen by a combination of microbeads and flow cytometry. Briefly, the murine splenic cell suspension was incubated with biotin-binding antibodies (anti-CD21/CD35, anti-Ter-119, anti-CD45R, anti-CD3, anti-CD11b, and anti-CD49; Miltenyi Biotec) to enrich lineage negative cells. The enriched lineage negative cells were further stained with FITC-lineage, PE-CD90.2 and APC-KLRG1

(Biolegend) and then sorted by flow cytometry. The purity of the sorted ILC2s was approximately 90% and the sorted ILC2s were cultured in RPMI 1640 medium supplemented with 10% FBS, 10 ng/ml IL-7, 10 ng/ml IL-33 (Peprotech), 10 U/ml penicillin and 10 U/ml streptomycin.

Flow cytometry analysis

Tumor tissues were minced and incubated in digestion solution containing 0.5 mg/ml collagenase V, 0.2 mg/ml hyaluronidase and 0.015 mg/ml DNase I (Sigma, St. Louis, USA) in a 37 °C water bath for 1 h. The samples were then filtered through a 70 μm strainer before staining with fluorescence antibodies. Mouse Percy5-CD45, FITC-lineage, PE-CD90.2, and APC-KLRG1 (Biolegend) were used to analyze the percentage of ILC2s in the mouse tumor tissue and human Percy5-CD45, FITC-lineage, PE-CRTH2, and APC-CD127 (Biolegend) were used to analyze the percentage of ILC2s in the human tumor tissue. Mouse CD8 cells were stained with Percy5-CD45, FITC-CD3, and PE-CD8 (Biolegend). For analyzing the percentage of MDSCs, FITC-CD11b and APC-Gr-1 (Biolegend) were used. All surface stained samples were kept at 4 °C for 30 min.

For intracellular staining of IL-9, tumor tissue single-cell suspensions were first stimulated with 50 ng/mL phorbol myristate acetate (PMA), 1 μg/mL ionomycin, and 2 μg/mL monensin (eBioscience, San Diego, USA) for 6 h. Samples were fixed, permeabilized, and stained with IL-9 antibody on a shaker at 4 °C for 45 min.

The apoptosis kit FITC-Annexin V and APC-7-AAD (Multisciences, Hangzhou, China) was used following the manufacturer's protocols to analyze the apoptosis of CT26 cells.

Immunofluorescence analysis

The frozen sections were incubated at room temperature for 1 hour and treated with 4% paraformaldehyde for 20 min. Sections were then washed three times with 1 × PBS and incubated with primary antibodies anti-lineage and anti-CRTH2 at a dilution of 1:200 in blocking buffer (PBS with 5% BSA, 1% saponin and 1% Triton 100) at 4 °C overnight. The sections were then washed three times in 1 × PBS and incubated with DAPI (1:1000; eBioscience) for 30 min, followed by three more washes in 1 × PBS. Neutral resin was used to seal the sections, which were left to air dry. Sections were then visualized directly with a confocal microscope.

Enzyme-linked immunosorbent assay (ELISA)

IFN-γ, IL-5, IL-9 and IL-13 in mouse serum and IFN-γ in culture supernatant were measured using an ELISA kit (MultiSciences) following the manufacturer's protocols. All samples were measured in triplicate and the mean concentration was calculated from the standard curve.

Cell proliferation assays

IL-9-stimulated CT26 cells were cultured in 96-well plates (8×10^3 cells/well) in 5% CO_2 at 37 °C for 24 h. The proliferation ability of CT26 cells was detected using a MTT proliferation assay kit (MultiSciences) as recommended by the manufacturer.

Migration assay

For the tumor migration assay, 2×10^5 IL-9-stimulated $CD8^+$ T cells were co-cultured with 1×10^5 CT26 cells in wells of a 24-well plate for 24 h. Adherent CT26 cells were collected and 2×10^4 cells in 0.2 ml of serum-free medium were added to the upper chamber of a transwell system; the lower chamber was filled with 0.6 ml serum-containing culture medium. The plate was incubated in 5% CO_2 at 37 °C for 20 h, and then the chamber was removed and cells were fixed with 4% paraformaldehyde for 15 min and stained with purple crystal for 10 min. Migration ability was quantified using direct microscopic visualization and cell counting.

Gene Expression Profiling Interactive Analysis (GEPIA)

GEPIA was used to analyze the expression of CXCL16 and CCL25 genes in the CRC tissue and adjacent normal tissue.

Statistical analysis

GraphPad Prism Version 7 software (GraphPad Software, Inc., La Jolla, CA, USA) was used to analyze all the data. The data are expressed as the mean ± SD. Comparisons between groups were assessed by unpaired Student's t-test or analysis of variance (ANOVA). A P value less than 0.05 was considered to indicate a statistically significant difference.

Results

1. ILC2s were significantly increased in the tumor tissue of the CRC mouse model and the CRC patient

Previous studies have shown that ILC2s can regulate the development of a variety of tumors[12]. However, the role of ILC2s in CRC has not been investigated. We first measured the percentage of ILC2s in the tumor and adjacent normal tissue of the CRC mouse model and CRC patient. We regarded Lin^- $CD90.2^+$ $KLRG1^+$ cells as mouse ILC2s and Lin^- $CD127^+$ $CRTH2^+$ cells as human ILC2s[15, 35]. Flow cytometry results showed that the percentage of ILC2s in mouse CRC tissue was significantly increased ($P < 0.001$) compared with that in adjacent normal tissue (Fig. 1A). We observed the similar result in the human CRC samples (Fig. 1B). The immunofluorescence result further demonstrated that ILC2s were increased in the human CRC tissue compared with adjacent normal tissue (Fig. 1C). Together, these results demonstrated that ILC2s were increased in the tumor tissue of the CRC mouse model and CRC patient.

2. Blocking ILC2s promoted tumor growth in CT26 cell-bearing mice

To investigate the role of ILC2s in the progression of CRC, we used the murine CRC cell line CT26 to generate a CRC tumor model. Five days after CT26 cells were implanted, anti-CD90.2, an ILC2 blocking antibody was intravenously injected for 5 consecutive days (Fig. 2A). The tumor volume was measured every 5 days and the tumor growth curves were drawn. The results showed that the tumor size was larger in anti-CD90.2-treated mice than control mice (Fig. 2B). In addition, the tumor volume and tumor weight were also increased in anti-CD90.2-treated mice (Fig. 2C,D).

We next measured the percentage of ILC2s in the spleen and tumor tissue from mice treated with anti-CD90.2 and control group. ILC2s were decreased both in the spleen and tumor tissue of the anti-CD90.2 group (Fig. 2E,F). We also examined the levels of ILC2-related cytokines IL-5, IL-9, and IL-13, and the antitumor cytokine IFN-γ in peripheral blood serum. ILC2-derived cytokines, IL-5, IL-9 and IFN-γ were decreased in the anti-CD90.2 group compared with the control group, but no significant change in IL-13 were found (Fig. 2G). It was suggested that the reduction in ILC2s could lead to an aggravation of tumor growth.

To preliminary examine the mechanism of increased tumor growth caused by reduced ILC2s, we detected the percentage of myeloid-derived suppressor cells (MDSCs) and $CD8^+$ T cells in the tumor tissues of mice from the anti-CD90.2 and control groups. The anti-CD90.2 group showed an increased percentage of MDSCs and decreased percentage of $CD8^+$ T cells in the tumor tissues compared with controls (Fig. 2H,I). Together, these results indicated that increased ILC2s exerted an anti-tumor role in CT26 cell-bearing mice and these effects might be through regulating the number of MDSCs and $CD8^+$ T cells.

3. IL-9 inhibited the growth of CT26 cells by activating $CD8^+$ T cells

Our findings indicated that ILC2s exerted anti-tumor effect in CRC. Previous studies have shown that IL-9, a cytokine secreted by ILC2s, has a powerful anti-tumor effect in solid tumors[36]. To examine the role of IL-9 in CRC, we stimulated CT26, CRC cell line, with IL-9 and then measured the effects on apoptosis and proliferation. The results showed that IL-9 at all tested concentrations had no significant effect on the apoptosis and proliferation of CT26 cells (Fig. 3A,B).

Previous studies showed that IL-9, a T-cell growth factor, regulated tumor progression by activating $CD8^+$ T cells[36]. We sorted $CD8^+$ T cells from tumor tissue and stimulated cells with IL-9. A greatly enhanced IFN-γ secretion ability was observed in $CD8^+$ T cells after stimulation by the various concentrations of IL-9 (Fig. 3C). Next, we co-cultured IL-9-stimulated $CD8^+$ T cells with CT26 cells for 24 h and then performed migration assays. The results showed that IL-9-stimulated $CD8^+$ T cells inhibited the migration ability of CT26 cells (Fig. 3D). The CT26 cell number was also decreased after co-culture with IL-9-stimulated $CD8^+$ T cells compared with controls (Fig. 3E). This result indicated that IL-9-stimulated $CD8^+$ T cells inhibited the proliferation of CT26 cells.

Apoptosis assay found that $CD8^+$ T cells promoted the apoptosis of CT26 cells, and IL-9-stimulated $CD8^+$ T cells further promoted the apoptosis of CT26 cells compared with $CD8^+$ T cells (Fig. 3F,G). These results demonstrated that IL-9 did not directly affect the biological activities of CT26 cells, but it could inhibit the proliferation, migration and apoptosis of CT26 cells via activating $CD8^+$ T cells in vitro. These findings indicated an anti-tumor function of IL-9 in the CRC tumor microenviroment.

4. Anti-IL-9 promoted tumor growth of CT26 cell-bearing mice but IL-9 inhibited tumor growth

Our findings indicated an anti-tumor effect of IL-9 on CT26 cells in vitro. To examine the anti-tumor effect of IL-9 in vivo, we established CT26 cell-bearing mice. At 5 days after tumor implantation, mice were injected intravenously with IL-9 or anti-IL-9 for 5 consecutive days (Fig. 4A). The results showed that neutralizing IL-9 promoted tumor growth in CT26 cell-bearing mice, while the tumor size and weight in the IL-9-treated group were decreased compared with the control group(Fig. 4B,C). These results demonstrated that IL-9 also exhibits anti-tumor effects in vivo.

To determine if IL-9 affected the tumor growth of CT26 cell-bearing mice by regulating $CD8^+$ T cells, we analyzed the percentage of $CD8^+$ T cells in tumor tissue with flow cytometry. The results showed that the percentage of $CD8^+$ T cells in the anti-IL-9 group was significantly decreased compared with controls, while IL-9 increased the percentage of $CD8^+$ T cells (Fig. 4D,E). We next measured the percentage of ILC2s in tumor tissues. We found the same result as the percentage of $CD8^+$ T cells in tumor tissues (Fig. 4F,G). Previous studies have shown that IL-9 promotes the growth and proliferation of ILC2s[37]. This finding is consistent with our results, which showed that neutralizing IL-9 reduced the number of ILC2s, while administrating IL-9 increased ILC2 numbers. Together, these results demonstrated that IL-9 regulates the number of $CD8^+$ T cells to regulate the CRC development.

5. ILC2 is the major IL-9-producing cell subset in murine CRC

To determine whether ILC2s exert anti-tumor effects on CRC through secreting IL-9, we used flow cytometry to analyze $IL\text{-}9^+$ cells in murine CRC tissue. More than half of the $IL\text{-}9^+$ cells were $lineage^-$ cells and almost all the $lineage^-$ cells were $CD90.2^+$ and $KLRG1^+$ cells (Fig. 5A). This result indicated that ILC2s were the major IL-9-producing cell-subset in murine CRC tissue (Fig. 5B). These findings also demonstrated that ILC2s could exert anti-tumor effects by secreting IL-9.

To clarify if ILC2s activate $CD8^+$ T cells through IL-9 to inhibit CRC progression. We sorted ILC2s and co-cultured ILC2s with $CD8^+$ T cells. ELISA result showed that ILC2s significantly increased the secretion of IFN-γ by $CD8^+$ T cells. However, when anti-IL-9 was added, the IFN-γ-secreting ability of $CD8^+$ T cells was decreased compared with the control group (Fig. 5C). This result further proved that ILC2s could inhibit the progression of CRC through secreting IL-9.

6. IL-9 reversed the tumor-promoting effects of blocking ILC2s

We demonstrated that ILC2s inhibit the progression of CRC by secreting IL-9. We next evaluated whether the tumor-promoting effect that results from blocking ILC2s could be reversed by IL-9. We generated CT26 cell-bearing mice and 5 days after tumor implantation, mice were injected intravenously with anti-CD90.2, and 30 min later, each IL-9 treatment group mouse also received IL-9 for 5 consecutive days (Fig. 6A). The results showed that IL-9 significantly inhibited tumor growth after ILC2s were blocked. The tumor size and weight were significantly reduced in the anti-CD90.2 plus IL-9 treatment group compared with the anti-CD90.2 group (Fig. 6B,C). In addition, the percentages of $CD8^+$ T cells and ILC2s in the anti-CD90.2 plus IL-9 treatment group were increased compared with the anti-CD90.2 group (Fig. 6D,E). These results further demonstrated that ILC2s regulate the progression of CRC by secreting IL-9, which could reverse the tumor-promoting effect that results from blocking ILC2s.

7. Peripheral ILC2s were recruited to the tumor site in CRC

Our results suggest that during the development of CRC, the body's immune resistance mechanism would result in increasing ILC2s, leading to inhibition of tumor growth by ILC2-mediated secretion of IL-9. However, we found that the percentage of ILC2s was decreased in the spleen of CT26 cell-bearing mice and CRC mice compared with control mice (Fig. 7A,B). This result was also observed in the peripheral blood of the CRC patient (Fig. 7C). We wondered why ILC2s were decreased in peripheral while increased in CRC tissue. Previous studies showed that ILC2s express the chemokine receptor CCR9 and CXCR6, which mediate the accumulation of ILC2s[38]. Li et al. demonstrated that CXCL16, a ligand of CXCR6, exerts a powerful chemoattractant effect to CXCR6-expressing ILC2s[39]. We thus used GEPIA to predict the expression of CCL25, the ligand of CCR9, and CXCL16 in CRC tissue. The results revealed no significant difference in the expression of CCL25 in CRC tissue and adjacent normal tissue, while the expression of CXCL16 was significantly increased in CRC tissue compared with adjacent normal tissue (Fig. 7D). These results indicated that decreased ILC2s in the peripheral may be due to the increased CXCL16 in CRC tissue. Together, these results suggest that the peripheral ILC2s may be recruited by CXCL16 to CRC tissue to exert anti-tumor effects.

Discussion

Current studies have shown that ILC2s are involved in the development of a variety of tumors in a tumor-specific manner[40]. However, the role of ILC2s in CRC has not been investigated. Reports have shown that the function of ILC2s in tumors depends on the cytokines that are secreted, and the roles of ILC2-derived IL-4, IL-5 and IL-13 in cancers have been previously reported[15, 41, 42]. The function of IL-9, a characteristic cytokine of ILC2s in tumors has not been examined[43]. Here we revealed that ILC2s are recruited to CRC tissue and secrete IL-9 to activate $CD8^+$ T cells, leading to inhibition of CRC development.

In this study, we observed increased ILC2s in tumor tissue compared with adjacent normal tissue in CRC mice. This is consistent with most previous studies showing that ILC2s are increased in tumor sites[15]. Previous studies have shown that there may be a large number of pro-inflammatory cytokines such as IL-33 and IL-25 in the tumor microenvironment[44]. Pro-inflammatory cytokines can lead to activation and proliferation of ILC2s[45, 46]. To investigate the function of the increased ILC2s in CRC, we used anti-CD90.2, an ILC2 blocking antibody, to determine the role of ILC2s in CT26 cell-bearing mice. Tumor growth was significantly increased in CT26 cell-bearing mice treated with anti-CD90.2, indicating that ILC2s serve an anti-tumor role in CRC. However, anti-CD90.2 is not an ILC2-specific neutralizing antibody, this is an limitation of our research. Our subsequent experiments with specific knockout of ILC2s are required to verify our results.

After showing that blocking ILC2s exacerbated CRC development, we investigated the anti-tumor mechanism of ILC2. IL-9, a characteristic cytokine of ILC2s, plays a positive role in the antitumor immunity of solid tumors. As a lymphoid cell growth factor, IL-9 directly inhibits tumor growth by up-regulating TRAF6 and Eomes and also indirectly inhibits the development of solid tumors by activation of $CD8^+$ T cells and mast cells[31–33]. Several studies have shown a role for Th9 cells, IL-9-skewed $CD8^+$ T (Tc9) cells, mast cells, and Vδ2 T cell-derived IL-9 in one or more tumor types[24, 47–49]. However, the role of ILC2-derived IL-9 has remained unclear. We found that that IL-9 had no effect on the apoptosis and proliferation of CT26 cells. However, IL-9-stimulated $CD8^+$ T cells significantly inhibited the migration, proliferation and apoptosis of CT26 cells. These results demonstrate an anti-tumor role of IL-9 in CRC. To demonstrate that the anti-tumor role of ILC2s was due to the secretion of IL-9 in CRC, we investigated the IL-9-secreting cells in CRC and found that ILC2s were the main IL-9-secreting cell subset. These results demonstrated that ILC2s inhibit the progression of CRC by secreting IL-9.

We next investigated the anti-tumor role of ILC2-derived IL-9 in the CT26 cell-bearing murine model in vivo. Intravenous injection ofIL-9 in mice exerted a powerful anti-tumor effect while injection of anti-IL-9 in mice promoted tumor growth. These findings demonstrate the anti-tumor role of IL-9 in CRC. Next, we examined whether IL-9 could rescue the tumor-promoting effect caused by ILC2 blocking. We used the CT26 cell-bearing mice model and found that IL-9 reversed the tumor-promoting role of ILC2s blocking. This result proved that ILC2s indeed exhibit a tumor suppressive function by producing IL-9 in CRC. However, these experiments have a limitation.We should use the mice CRC model to detect the role of ILC2s and IL-9 rather than just used the CT26-bearing mice model. In our next study, we plan to investigate the role of ILC2s and IL-9 in a CRC model.

In our research, we found that ILC2s was decreased in the peripheral of the CRC model. Previous studies demonstrated that ILC2s express the chemokine receptors CCR6 and CXCR6 and can be recruited to tissues that highly expressed CCL25 and CXCL16[38]. Based on these data and the increased ILC2s in CRC tissue, we examined whether CRC tissue highly expressed chemokines CCL25 and CXCL16. GEPIA results showed that CXCL16 is highly expressed in CRC tissues compared with adjacent normal tissues. This result explains the decrease of ILC2s in peripheral and increase in tumor tissue of CRC and further

suggests the possibility that ILC2s may migrate from the periphery to CRC tissue by chemotaxis induced by CXCL16.

Conclusions

In this study, we demonstrated the role of ILC2s and ILC2-derived IL-9 in CRC. We found that ILC2s were increased in CRC tissue, and it was a main IL-9-secreting cell-subset. ILC2s inhibited the growth of CRC by secreting IL-9. We also found that that the CXCL16 was increased in CRC tissue and may recruit peripheral ILC2s to CRC tissue to exert anti-CRC effect.

Abbreviations

ILC2s: type 2 innate lymphoid cells; IL-9: interleukin-9; CRC: colorectal cancer; Th9: T-helper9; IL-9R: IL-9 receptor; ELISA: enzyme-linked immunosorbent assay; GEPIA: Gene Expression Profiling Interactive Analysis

Declarations

Funding

This work was supported by the National Natural Science Foundation of China (grant no. 81771756, 81871244), Social Development Project of Jiangsu Province (grant no. BE2016716), and the Doctorial Innovation Foundation of Jiangsu Province (grant no. KYCX17_1816).

Conflict of interests

The authors declare that there are no conflicts of interest.

Author contribution

JW, LH and YQW performed the experiments, analyzed the data, and wrote the original draft; XYJ, MH, WC, JJC and HXW performed data curation and formal analysis; DKK and VA analyzed the data with software; SY contributed to the language editing; CXS collected the patient CRC samples; and ZLS, HX, and SW were responsible for the study design, visualization, and editing the manuscript. All authors approved the final version of the manuscript.

Acknowledgements

We thank Liwen Bianji, Edanz Editing China (www.liwenbianji.cn/ac), for editing the English text of a draft of this manuscript.

Ethics approval and consent to participate

All animal experiments were complied with the protocol of Jiangsu University Animal Ethics and Experimentation Committee.

References

1. Thomas H. Colorectal cancer: CRC endothelial regulation. Nat Rev Gastroenterol Hepatol. 2016;13:682.
2. Boselli C, Cirocchi R, Gemini A, Grassi V, Avenia S, Polistena A, Sanguinetti A, Burattini MF, Pironi D, Santoro A, et al. Surgery for colorectal cancer in elderly: a comparative analysis of risk factor in elective and urgency surgery. Aging Clin Exp Res. 2017;29:65–71.
3. Duan X, Chan C, Han W, Guo N, Weichselbaum RR, Lin W. Immunostimulatory nanomedicines synergize with checkpoint blockade immunotherapy to eradicate colorectal tumors. Nat Commun. 2019;10:1899.
4. Dewson G, Silke J. The Walrus and the Carpenter: Complex Regulation of Tumor Immunity in Colorectal Cancer. Cell. 2018;174:14–6.
5. Simoni Y, Fehlings M, Kloverpris HN, McGovern N, Koo SL, Loh CY, Lim S, Kurioka A, Fergusson JR, Tang CL, et al. Human Innate Lymphoid Cell Subsets Possess Tissue-Type Based Heterogeneity in Phenotype and Frequency. Immunity. 2017;46:148–61.
6. Ercolano G, Falquet M, Vanoni G, Trabanelli S, Jandus C. ILC2s: New Actors in Tumor Immunity. Front Immunol. 2019;10:2801.
7. Schwartz C, Khan AR, Floudas A, Saunders SP, Hams E, Rodewald HR, McKenzie ANJ, Fallon PG. ILC2s regulate adaptive Th2 cell functions via PD-L1 checkpoint control. J Exp Med. 2017;214:2507–21.
8. Zhu P, Zhu X, Wu J, He L, Lu T, Wang Y, Liu B, Ye B, Sun L, Fan D, et al. IL-13 secreted by ILC2s promotes the self-renewal of intestinal stem cells through circular RNA circPan3. Nat Immunol. 2019;20:183–94.
9. Ghaedi M, Shen ZY, Orangi M, Martinez-Gonzalez I, Wei L, Lu X, Das A, Heravi-Moussavi A, Marra MA, Bhandoola A, Takei F. **Single-cell analysis of RORalpha tracer mouse lung reveals ILC progenitors and effector ILC2 subsets**. *J Exp Med* 2020, 217.
10. Hammad H, Lambrecht BN. Barrier Epithelial Cells and the Control of Type 2 Immunity. Immunity. 2015;43:29–40.
11. Bouchery T, Le Gros G, Harris N. ILC2s-Trailblazers in the Host Response Against Intestinal Helminths. Front Immunol. 2019;10:623.
12. Wan J, Cai W, Wang H, Cheng J, Su Z, Wang S, Xu H. Role of type 2 innate lymphoid cell and its related cytokines in tumor immunity. J Cell Physiol. 2020;235:3249–57.
13. Moral JA, Leung J, Rojas LA, Ruan J, Zhao J, Sethna Z, Ramnarain A, Gasmi B, Gururajan M, Redmond D, et al. ILC2s amplify PD-1 blockade by activating tissue-specific cancer immunity. Nature. 2020;579:130–5.

14. Zhang MZ, Wang X, Wang Y, Niu A, Wang S, Zou C, Harris RC. IL-4/IL-13-mediated polarization of renal macrophages/dendritic cells to an M2a phenotype is essential for recovery from acute kidney injury. Kidney Int. 2017;91:375–86.
15. Trabanelli S, Chevalier MF, Martinez-Usatorre A, Gomez-Cadena A, Salome B, Lecciso M, Salvestrini V, Verdeil G, Racle J, Papayannidis C, et al. Tumour-derived PGD2 and NKp30-B7H6 engagement drives an immunosuppressive ILC2-MDSC axis. Nat Commun. 2017;8:593.
16. Liou GY, Bastea L, Fleming A, Doppler H, Edenfield BH, Dawson DW, Zhang L, Bardeesy N, Storz P. The Presence of Interleukin-13 at Pancreatic ADM/PanIN Lesions Alters Macrophage Populations and Mediates Pancreatic Tumorigenesis. Cell Rep. 2017;19:1322–33.
17. Monticelli LA, Osborne LC, Noti M, Tran SV, Zaiss DM, Artis D. IL-33 promotes an innate immune pathway of intestinal tissue protection dependent on amphiregulin-EGFR interactions. Proc Natl Acad Sci U S A. 2015;112:10762–7.
18. Kim J, Kim W, Moon UJ, Kim HJ, Choi HJ, Sin JI, Park NH, Cho HR, Kwon B. Intratumorally Establishing Type 2 Innate Lymphoid Cells Blocks Tumor Growth. J Immunol. 2016;196:2410–23.
19. Saranchova I, Han J, Zaman R, Arora H, Huang H, Fenninger F, Choi KB, Munro L, Pfeifer CG, Welch I, et al. Type 2 Innate Lymphocytes Actuate Immunity Against Tumours and Limit Cancer Metastasis. Sci Rep. 2018;8:2924.
20. Verma M, Liu S, Michalec L, Sripada A, Gorska MM, Alam R. Experimental asthma persists in IL-33 receptor knockout mice because of the emergence of thymic stromal lymphopoietin-driven IL-9(+) and IL-13(+) type 2 innate lymphoid cell subpopulations. J Allergy Clin Immunol. 2018;142:793–803.e798.
21. Vyas SP, Hansda AK, Kaplan MH, Goswami R. Calcitriol Regulates the Differentiation of IL-9-Secreting Th9 Cells by Modulating the Transcription Factor PU.1. J Immunol. 2020;204:1201–13.
22. Abdul Qayum A, Koh B, Martin RK, Kenworthy BT, Kharwadkar R, Fu Y, Wu W, Conrad DH, Kaplan MH. The Il9 CNS-25 Regulatory Element Controls Mast Cell and Basophil IL-9 Production. J Immunol. 2019;203:1111–21.
23. Wang W, Cheng ZS, Chen YF, Lin YH. Increased circulating IL-9-producing CD8(+) T cells are associated with eosinophilia and high FeNO in allergic asthmatics. Exp Ther Med. 2016;12:4055–60.
24. Peters C, Hasler R, Wesch D, Kabelitz D. Human Vdelta2 T cells are a major source of interleukin-9. Proc Natl Acad Sci U S A. 2016;113:12520–5.
25. Schwartz DM, Farley TK, Richoz N, Yao C, Shih HY, Petermann F, Zhang Y, Sun HW, Hayes E, Mikami Y, et al. Retinoic Acid Receptor Alpha Represses a Th9 Transcriptional and Epigenomic Program to Reduce Allergic Pathology. Immunity. 2019;50:106–20.e110.
26. Jiang W, Yuan X, Zhu H, He C, Ge C, Tang Q, Xu C, Hu B, Huang C, Ma T. Inhibition of Histone H3K27 Acetylation Orchestrates Interleukin-9-Mediated and Plays an Anti-Inflammatory Role in Cisplatin-Induced Acute Kidney Injury. Front Immunol. 2020;11:231.
27. Ciccia F, Guggino G, Ferrante A, Cipriani P, Giacomelli R, Triolo G. Interleukin-9 and T helper type 9 cells in rheumatic diseases. Clin Exp Immunol. 2016;185:125–32.

28. Zheng Y, He Y, Xiao M, Zhang W, Xia W, Hu H, Mao L, Liu A, Chen Z, Bai X, Li Y. Interleukin 9 prevents immune thrombocytopenia in mice via JAK/STAT5 signaling. Exp Cell Res. 2020;388:111801.
29. He Y, Dong L, Cao Y, Bi Y, Liu G. IL-9 and Th9 Cells in Tumor Immunity. Adv Exp Med Biol. 2020;1240:35–46.
30. Li HJ, Sun QM, Liu LZ, Zhang J, Huang J, Wang CH, Ding R, Song K, Tong Z. High expression of IL-9R promotes the progression of human hepatocellular carcinoma and indicates a poor clinical outcome. Oncol Rep. 2015;34:795–802.
31. Lu Y, Wang Q, Xue G, Bi E, Ma X, Wang A, Qian J, Dong C, Yi Q. Th9 Cells Represent a Unique Subset of CD4(+) T Cells Endowed with the Ability to Eradicate Advanced Tumors. Cancer Cell. 2018;33:1048–60.e1047.
32. Vegran F, Apetoh L, Ghiringhelli F. Th9 cells: a novel CD4 T-cell subset in the immune war against cancer. Cancer Res. 2015;75:475–9.
33. Purwar R, Schlapbach C, Xiao S, Kang HS, Elyaman W, Jiang X, Jetten AM, Khoury SJ, Fuhlbrigge RC, Kuchroo VK, et al. Robust tumor immunity to melanoma mediated by interleukin-9-producing T cells. Nat Med. 2012;18:1248–53.
34. Wang C, Lu Y, Chen L, Gao T, Yang Q, Zhu C, Chen Y. Th9 cells are subjected to PD-1/PD-L1-mediated inhibition and are capable of promoting CD8 T cell expansion through IL-9R in colorectal cancer. Int Immunopharmacol. 2020;78:106019.
35. Moro K, Ealey KN, Kabata H, Koyasu S. Isolation and analysis of group 2 innate lymphoid cells in mice. Nat Protoc. 2015;10:792–806.
36. Parrot T, Allard M, Oger R, Benlalam H, Raingeard de la Bletiere D, Coutolleau A, Preisser L, Desfrancois J, Khammari A, Dreno B, et al. IL-9 promotes the survival and function of human melanoma-infiltrating CD4(+) CD8(+) double-positive T cells. Eur J Immunol. 2016;46:1770–82.
37. Turner JE, Morrison PJ, Wilhelm C, Wilson M, Ahlfors H, Renauld JC, Panzer U, Helmby H, Stockinger B. IL-9-mediated survival of type 2 innate lymphoid cells promotes damage control in helminth-induced lung inflammation. J Exp Med. 2013;210:2951–65.
38. Kim MH, Taparowsky EJ, Kim CH. Retinoic Acid Differentially Regulates the Migration of Innate Lymphoid Cell Subsets to the Gut. Immunity. 2015;43:107–19.
39. Li Y, Chen S, Chi Y, Yang Y, Chen X, Wang H, Lv Z, Wang J, Yuan L, Huang P, et al. Kinetics of the accumulation of group 2 innate lymphoid cells in IL-33-induced and IL-25-induced murine models of asthma: a potential role for the chemokine CXCL16. Cell Mol Immunol. 2019;16:75–86.
40. Trabanelli S, Chevalier MF, Derre L, Jandus C. The pro- and anti-tumor role of ILC2s. Semin Immunol. 2019;41:101276.
41. Halim TYF, Rana BMJ, Walker JA, Kerscher B, Knolle MD, Jolin HE, Serrao EM, Haim-Vilmovsky L, Teichmann SA, Rodewald HR, et al. Tissue-Restricted Adaptive Type 2 Immunity Is Orchestrated by Expression of the Costimulatory Molecule OX40L on Group 2 Innate Lymphoid Cells. Immunity. 2018;48:1195–207.e1196.

42. Bie Q, Zhang P, Su Z, Zheng D, Ying X, Wu Y, Yang H, Chen D, Wang S, Xu H. Polarization of ILC2s in peripheral blood might contribute to immunosuppressive microenvironment in patients with gastric cancer. J Immunol Res. 2014;2014:923135.
43. Shik D, Tomar S, Lee JB, Chen CY, Smith A, Wang YH. IL-9-producing cells in the development of IgE-mediated food allergy. Semin Immunopathol. 2017;39:69–77.
44. Ameri AH, Moradi Tuchayi S, Zaalberg A, Park JH, Ngo KH, Li T, Lopez E, Colonna M, Lee RT, Mino-Kenudson M, Demehri S. IL-33/regulatory T cell axis triggers the development of a tumor-promoting immune environment in chronic inflammation. Proc Natl Acad Sci U S A. 2019;116:2646–51.
45. Frisbee AL, Saleh MM, Young MK, Leslie JL, Simpson ME, Abhyankar MM, Cowardin CA, Ma JZ, Pramoonjago P, Turner SD, et al. IL-33 drives group 2 innate lymphoid cell-mediated protection during Clostridium difficile infection. Nat Commun. 2019;10:2712.
46. von Moltke J, Ji M, Liang HE, Locksley RM. Tuft-cell-derived IL-25 regulates an intestinal ILC2-epithelial response circuit. Nature. 2016;529:221–5.
47. Ma X, Bi E, Huang C, Lu Y, Xue G, Guo X, Wang A, Yang M, Qian J, Dong C, Yi Q. Cholesterol negatively regulates IL-9-producing CD8(+) T cell differentiation and antitumor activity. J Exp Med. 2018;215:1555–69.
48. Rivera Vargas T, Humblin E, Vegran F, Ghiringhelli F, Apetoh L. TH9 cells in anti-tumor immunity. Semin Immunopathol. 2017;39:39–46.
49. Elieh Ali Komi D, Grauwet K. Role of Mast Cells in Regulation of T Cell Responses in Experimental and Clinical Settings. Clin Rev Allergy Immunol. 2018;54:432–45.

Figures

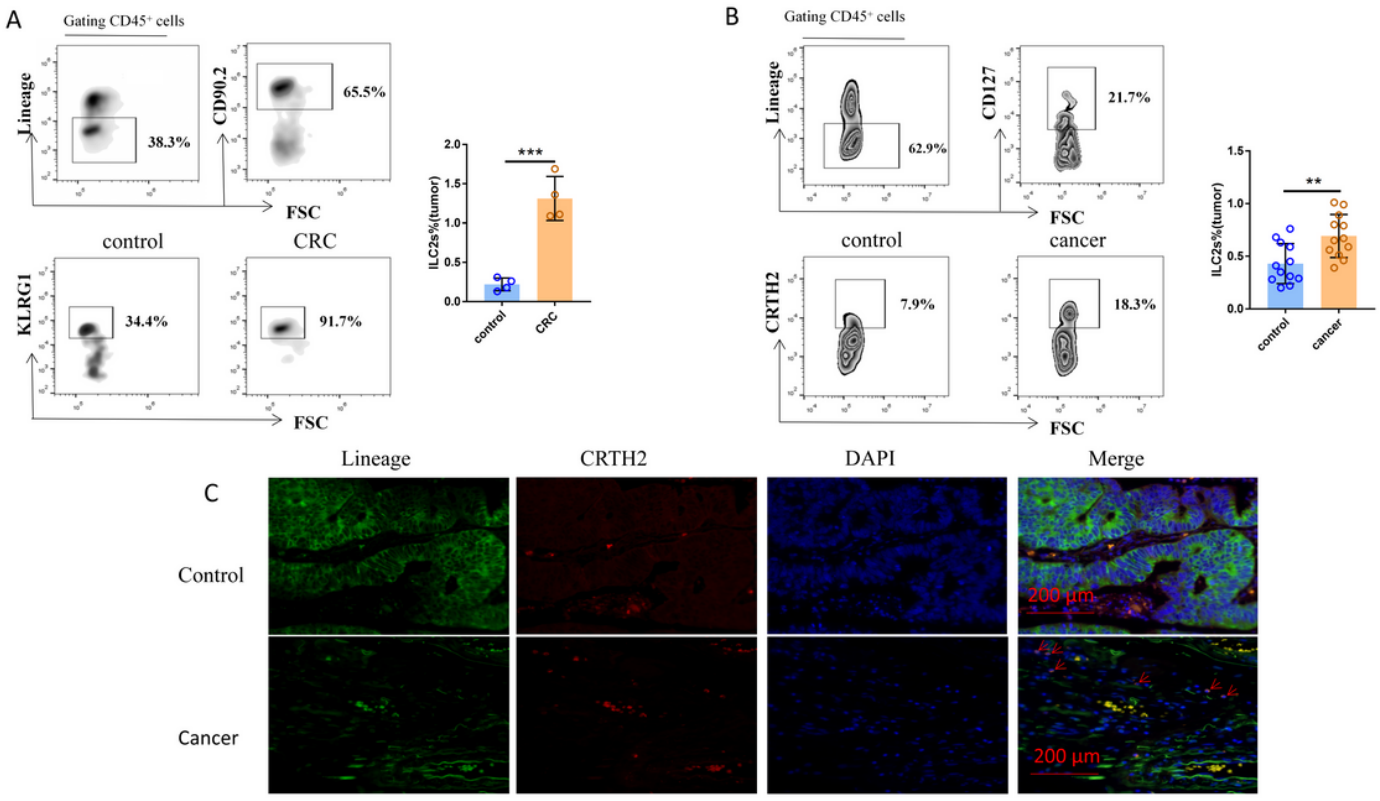

Figure 1

ILC2s were significantly increased in the tumor tissue of the CRC mouse model and the CRC patient. A, Flow cytometry was performed to detect the percentage of ILC2s (Lineage-CD90.2+KLRG1+) in the tumor and adjacent normal tissues of the CRC mice. B, Flow cytometry was performed to detect the percentage of ILC2s (Lineage-CD127+CRTH2+) in the tumor and adjacent normal tissues of the CRC patient. C, Immunofluorescence was performed to measure the ILC2s in the tumor and adjacent normal tissues of the CRC patient. Data are presented as mean±SD, *P < 0.005, **P < 0.001 compared with controls.

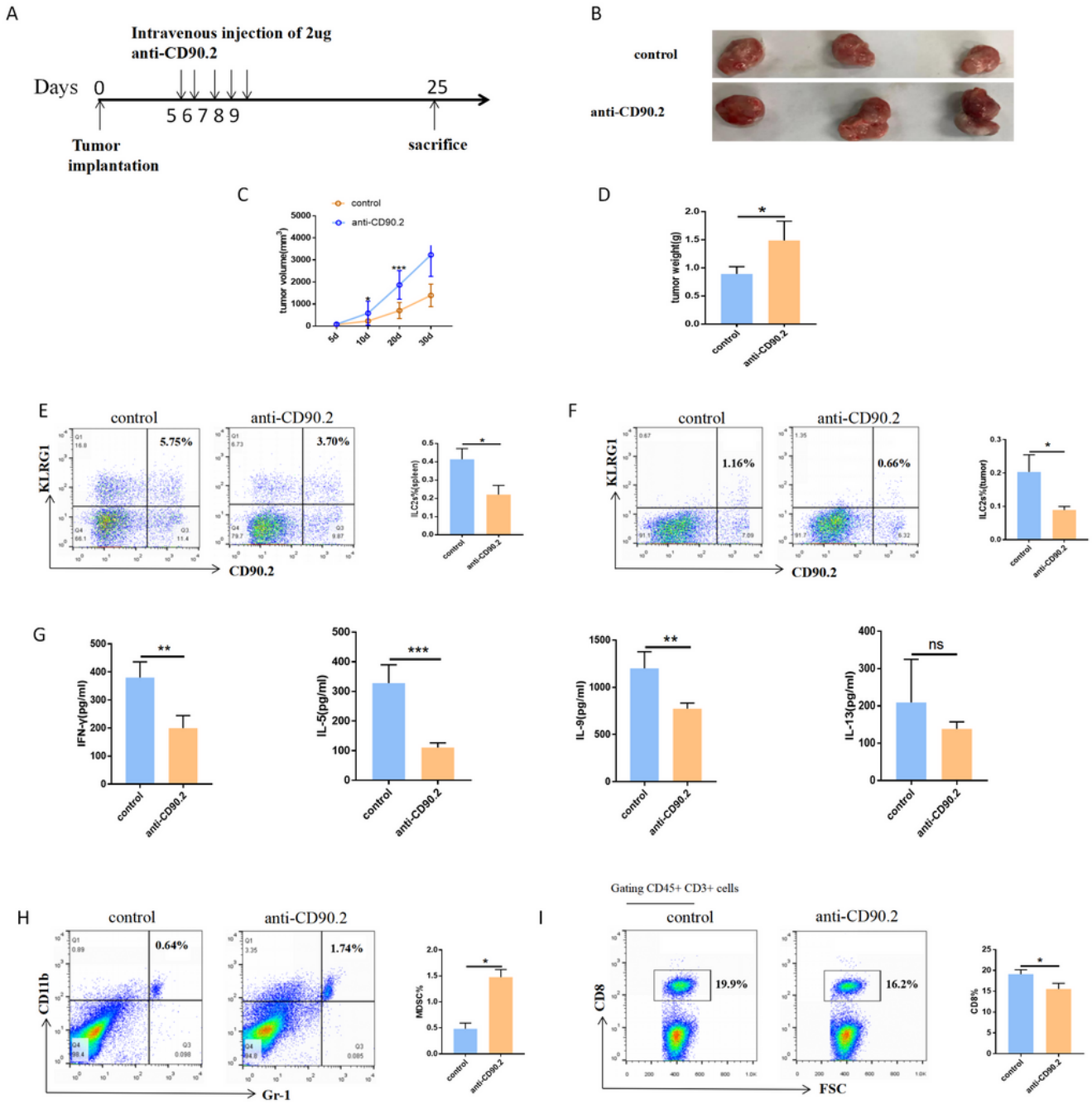

Figure 3

Blocking ILC2s promoted tumor growth in CT26 cell-bearing mice. A, Anti-CD902 was intravenously injected in CT26 cell-bearing mice for 5 consecutive days at a dose of 2 μg per mouse. B–D, Tumor volume and weight in the anti-CD90.2 and control group mice. E–F, Percentages of ILC2s in the spleen and tumors of anti-CD90.2 and control group mice were detected by flow cytometry. G, ILC2-related cytokines IL-5, IL-9, and IL-13 and antitumor cytokine IFN-γ were measured in peripheral blood serum by

ELISA. H–I, Percentages of CD11b+Gr-1+ MDSCs and CD8+ T cells in tumors were detected by flow cytometry. Data are presented as mean±SD, *P < 0.005, **P < 0.001 compared with controls.

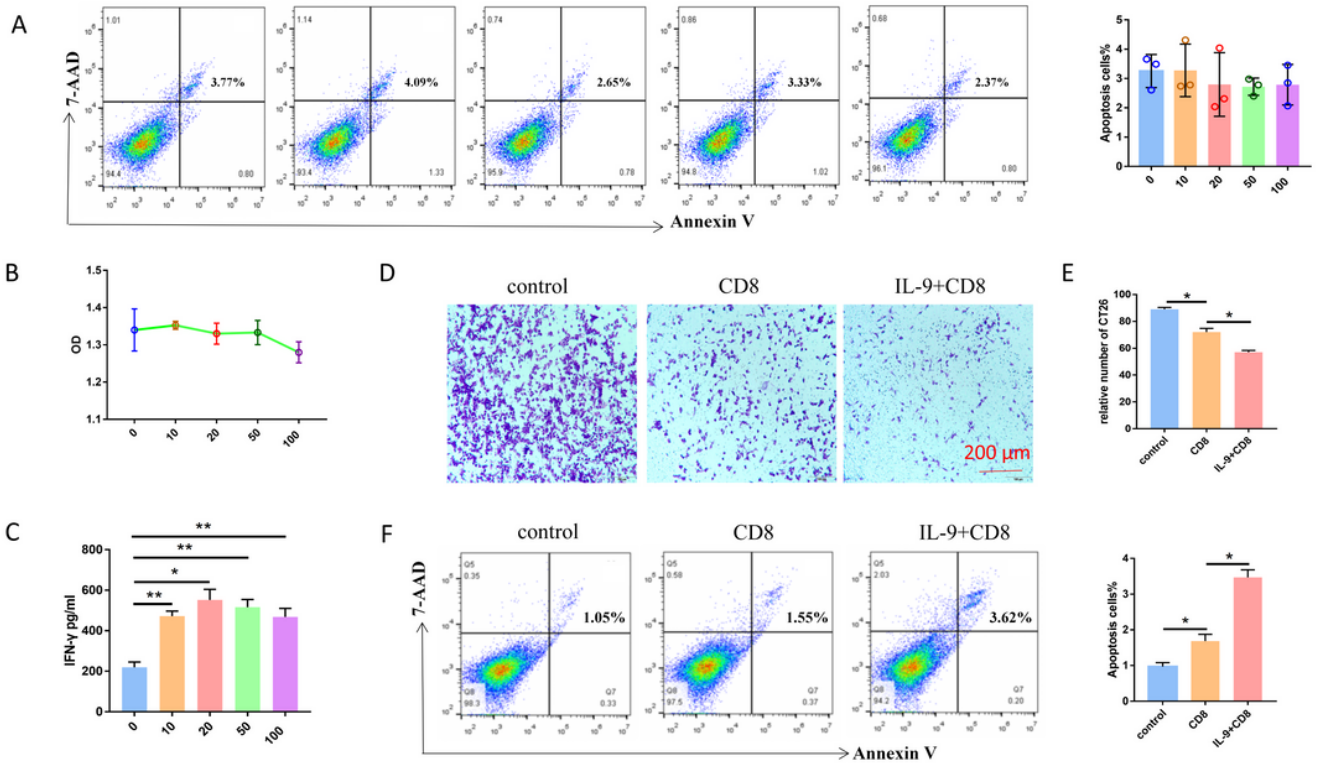

Figure 5

IL-9 inhibits the growth of CT26 cells through activating CD8+ T cells. A, Various concentrations of IL-9 were applied to stimulate 2×105 CT26 cells in a 24-well plate for 24 h, and flow cytometry was used to evaluate apoptosis. B, Various concentrations of IL-9 were applied to stimulate 5×103 CT26 cells in a 96-well plate for 36 h, and proliferation was examined by MTT proliferation assay. C, CD8+ T cells were isolated from tumor tissue using a tumor infiltration CD8+ T-cell magnetic bead sorting kit. CD8+ T cells (5×104) were stimulated by different concentrations of IL-9 in 96-well plates for 24 h and the secreted IFN-γ in the supernatant was measured by ELISA. D, IL-9-stimulated 2×105 CD8+ T cells were co-cultured with 1×105 CT26 cells in 24-well plates for 24 h. Adherent CT26 cells were collected and added to the upper chamber of a transwell system; the lower chamber was filled with 0.6 ml serum-containing culture medium. Cells were incubated for 18 h and the number of migrated CT26 cells was determined. E, The relative number of CT26 cells was measured after co-culturing with CD8+ T cells to determine the proliferation ability of CT26 cells. F, Apoptosis assay was performed to detect the apoptosis of CT26 cells after co-culturing with CD8+ T cells. Data are presented as mean±SD, *P < 0.005, **P < 0.001 compared with controls.

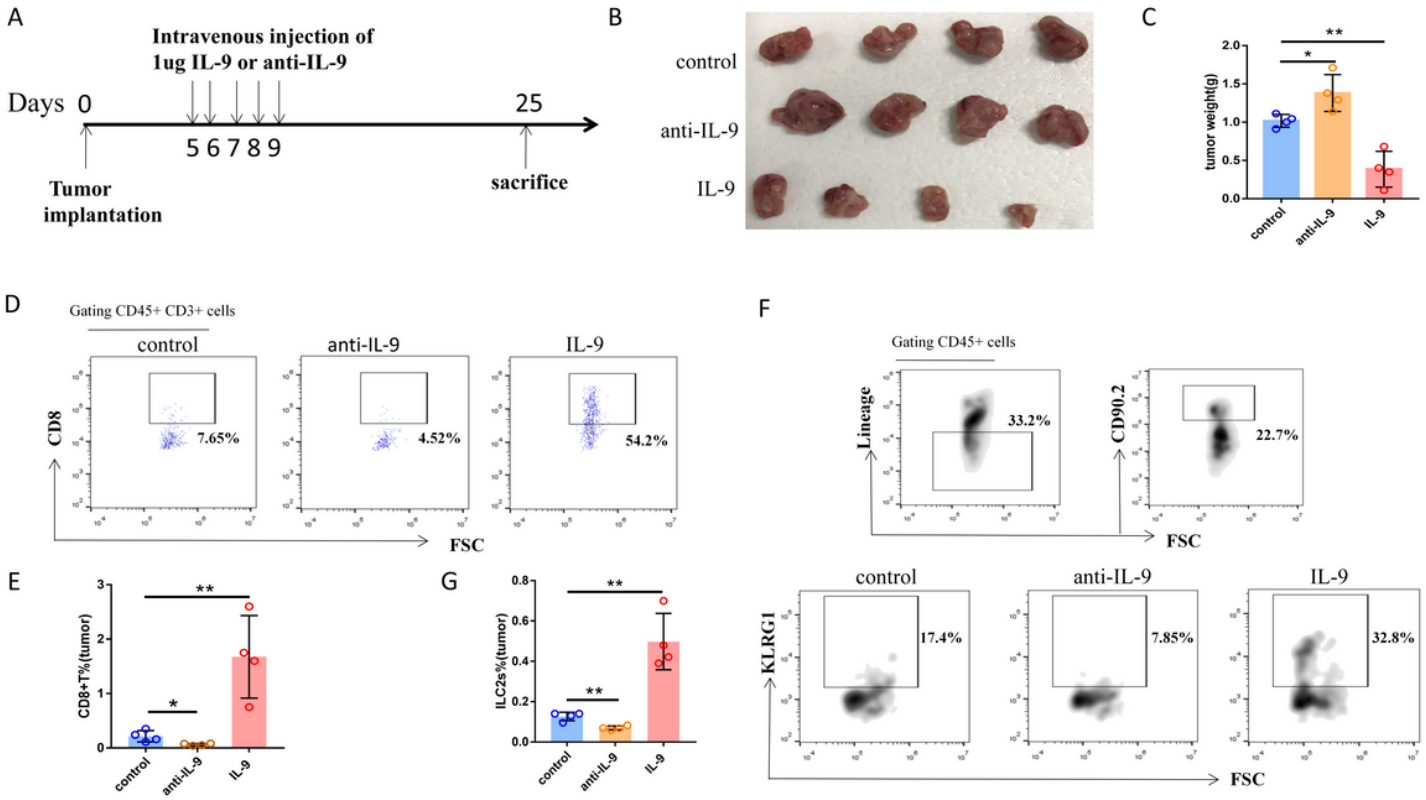

Figure 7

Anti-IL-9 promoted the tumor growth of CT26 cell-bearing mice but IL-9 inhibited tumor growth. A, At 5 days after CT26 cell implantation, mice were injected intravenously with 1 μg IL-9 or 5 μg anti-IL-9 for 5 consecutive days. B–C, Tumor volume and weight in the different treatment groups. D–E, The percentages of CD8+ T cells in the tumors of IL-9- and anti-IL-9-treated mice and control mice were detected by flow cytometry. F–G, The percentages of ILC2s in the tumors of IL-9- and anti-IL-9-treated mice and control mice were detected by flow cytometry. Data are presented as mean±SD, *P < 0.005, **P < 0.001 compared with controls.

A

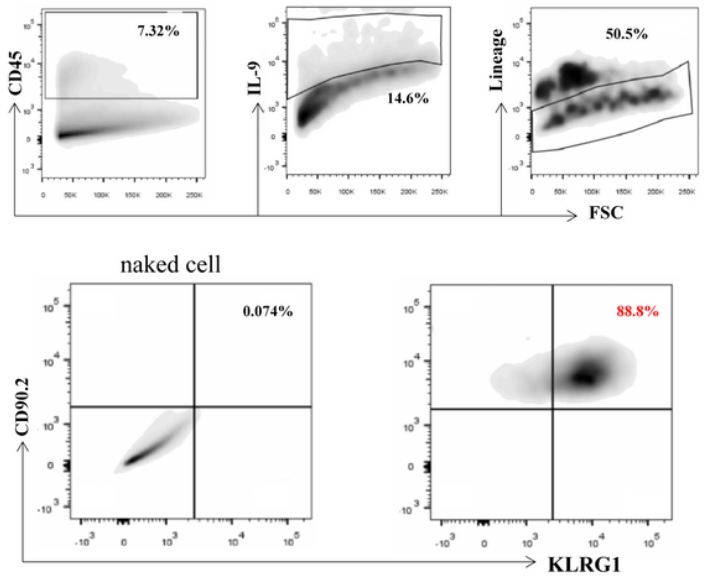

B

sample	1	2	3
ILC2s/IL-9+ cell%	44	52	58

C

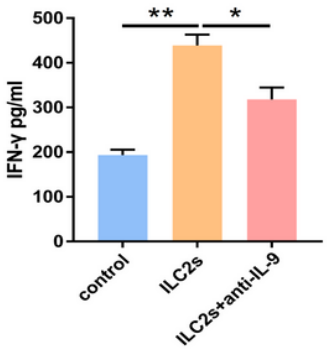

Figure 9

ILC2 is the major IL-9-producing cell subset in murine CRC. A, Representative examples of flow cytometry analysis of IL-9-producing ILC2s in CRC tissue. B, Percentages of IL-9-producing ILC2s/IL-9+ cells. C, CD8+ T cells were isolated from tumor tissue using a tumor infiltration CD8+ T-cell magnetic bead sorting kit. ILC2s were sorted from mouse spleen by a combination of magnetic bead and flow cytometry sorting. CD8+ T cells (1×105) were co-cultured with ILC2s (1×105)with/without anti-IL-9 for 3 days. ELISA was used to detect the secretion of IFN-γ in the supernatant. Data are presented as mean±SD, *P < 0.005, **P < 0.001 compared with controls.

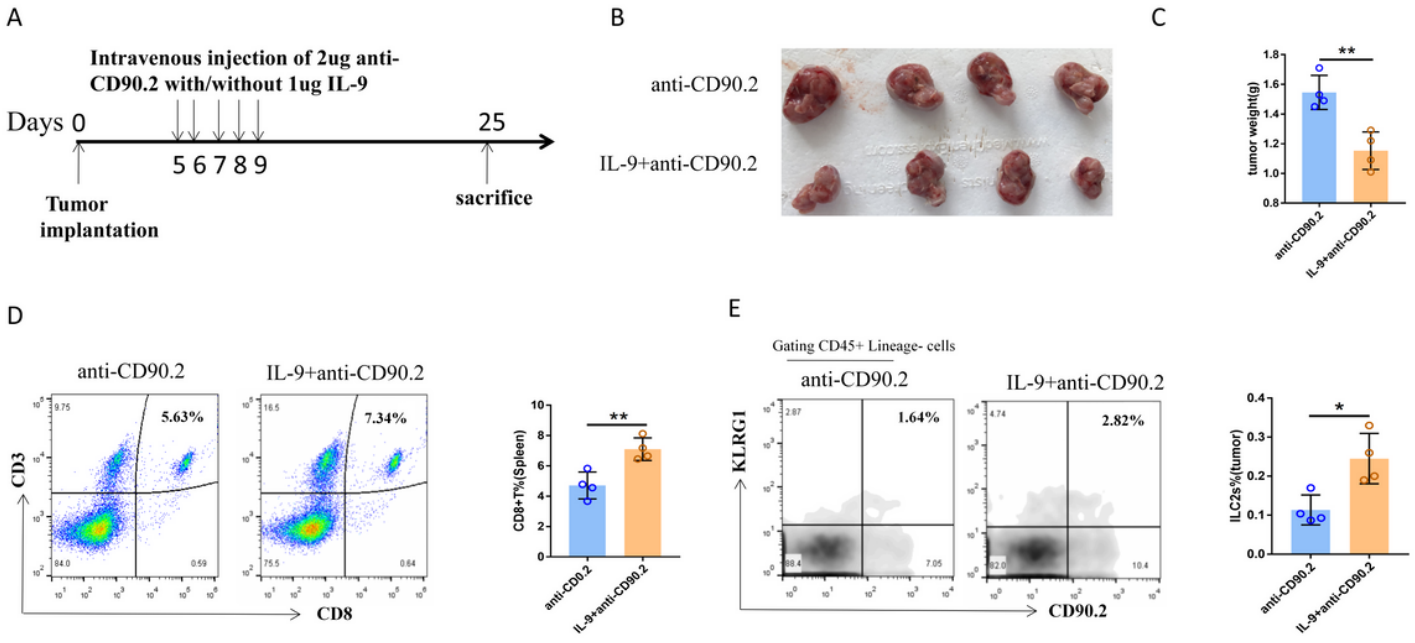

Figure 11

IL-9 reverses the tumor-promoting effect of blocking ILC2s. A, At 5 days after CT26 cell implantation, mice were injected intravenously with 2 μg anti-CD90.2 or 2 μg anti-CD90.2 plus 1 μg IL-9 for 5 consecutive days. B-C, Tumor volume and weight in different treatment groups. D, The percentage of CD8+ T cells in the tumors of anti-CD90.2-treated mice and anti-CD90.2 plus IL-9-treated mice was detected by flow cytometry. E, The percentage of ILC2s in the tumors of anti-CD90.2-treated and anti-CD90.2 plus IL-9-treated mice was detected by flow cytometry. Data are presented as mean±SD, *P < 0.005; **P < 0.001 compared with controls.

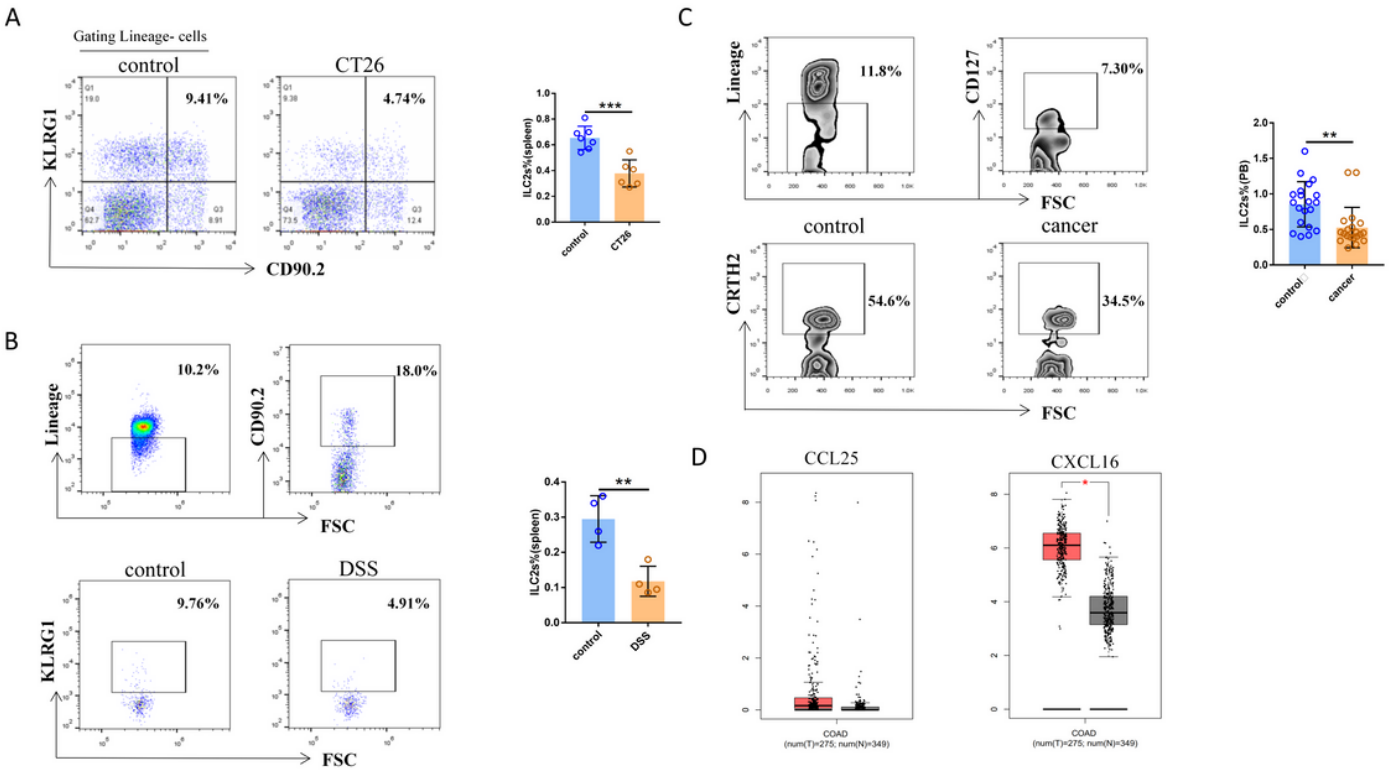

Figure 13

Peripheral ILC2s could be recruited to the tumor site in CRC. A, The percentage of ILC2s in the spleen of CT26-bearing mice and control mice was detected by flow cytometry. B-C, Flow cytometry was used to test the percentage of ILC2s in the tumor and adjacent normal tissues of CRC mice and CRC patient. D, GEPIA was used to analyze the expression of CCL25 and CXCL16 in the tumor and adjacent normal tissues of COAD. Data are presented as mean±SD, *P < 0.005; **P < 0.001 compared with controls.